Biophysical Chemistry, 39 (1991) 45–56
Elsevier

BIOCHE 01522

Induction of DNA bending by bifunctional intercalating agents of the 7H-pyridocarbazole family

R.C. Maroun and B.P. Roques

Laboratoire de Pharmacochimie Moléculaire (INSERM U266) and Laboratoire des Interactions Biologiques (CNRS UA498), Université René Descartes, Laboratoire de Chimie Organique, INSERM U266-CNRS UA498, 4, Avenue de l'Observatoire, 75270 Paris 06, France

Received 26 February 1990
Revised manuscript received 6 July 1990
Accepted 9 July 1990

DNA intercalation; DNA bending; Energy minimization; Antitumoral activity

The structures and binding energetics of selected complexes formed between the deoxynucleotides d(CpGpGpCpG)·d(CpGpCpCpG), d(CpGpApTpCpG)$_2$, d(GpCpGpCpCpG)·d(CpGpGpCpGpC), and d(CpGpCpCpCpG)$_2$ with the DNA bifunctional intercalating agent ditercalinium and three of its rigid linking chain derivatives have been investigated theoretically by means of a molecular mechanics approach that takes into account nucleic acid flexibility, ligand flexibility and solvent dielectric effects (R. Lavery, in: Unusual DNA structures, eds S. Harvey and R. Wells (Pergamon, New York, 1988) p. 189; R. Lavery, in: DNA bending and curvature, eds W.K. Olson et al. (Adenine Press, New York, 1988) p. 191). The piperidinium chains of the bis-intercalating ligands are always located in the major groove of DNA. For the energy-minimized complexes the ligand proceeds to bind following preferentially the 5′-pyrimidine-purine-3′ alternating sequence, thus dictating the number of internal exclusion sites. The complexes with three exclusion sites will present (i) a bending of the structure towards the major groove, and (ii) a non-ideal distribution of unwinding angles; complexes with less than three exclusion sites will remain essentially linear. The absence of a bend does not preclude other types of local deformations of the base-pairs such as inclination, buckle and tip. The proposed structures of the d(CpGpApTpCpG)$_2$ complexes are in agreement with NMR structural results. The possible relevance of these findings to a previously proposed mode of interaction for ditercalinium-like DNA ligands is discussed.

1. Introduction

In previous papers we have investigated by theoretical computations the intercalative binding of a 7H-pyrido[4,3-*c*]carbazole monomer to d(CG)$_2$ [3], and that of ditercalinium (denoted 2-0-2), a high-affinity DNA bis-intercalating agent endowed with antitumoral activity, to d(CGCG)$_2$ [4] (see ref. 5 for a review on polyfunctional DNA intercalating agents). In order to modulate this activity, a number of derivatives of ditercalinium in which one to three methylenes have been introduced between the piperidine rings of the rigid linking side chain have been synthetised. The distance separating the two planar heterocyclic rings is thus changed (fig. 1); the compounds are henceforth denoted 2-1-2, 2-2-2 and 2-3-2, respectively.

Among these rigid 7H-pyrido[4,3-*c*]carbazole dimers, 2-1-2 maintains nearly the activity of ditercalinium, whereas the cytotoxicity and related antitumoral properties decrease strongly for 2-2-2 and disappear for 2-3-2 [6] even though bis-intercalation is apparently preserved for all three compounds [6,7]. NMR techniques have been used to characterise and compare the complexes of 2-0-2,

Correspondence address: R.C. Maroun, Laboratoire de Pharmacochimie Moléculaire, 4, Ave de l'Observatoire, 75270 Paris 06, France.

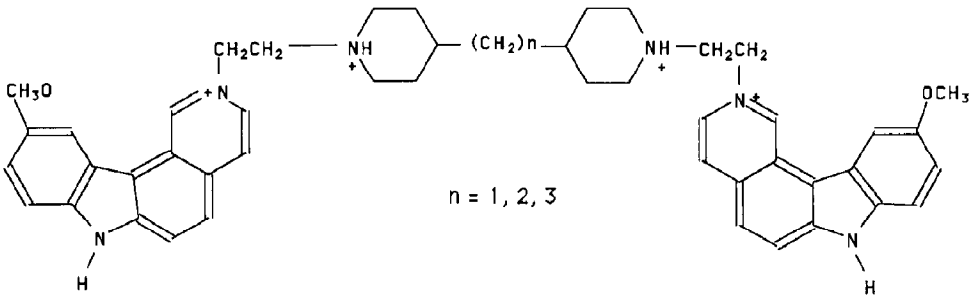

Fig. 1. Chemical structure of drugs.

2-2-2 and 2-3-2 with $d(CGATCG)_2$ in solution [8]. The results indicate that the 2-2-2 and 2-3-2 dimers form major groove complexes, with their chromophores occupying the terminal dCpdG sites of the oligohexanucleotide whereas 2-0-2 forms a major groove complex with one of the two chromophores fitting a terminal dCpdG site and the other the dApdT site. 2-1-2 induced precipitation when added to the same hexanucleotide.

In this paper we investigate, by means of theoretical computations the molecular structures and energetics of the complexes formed by intercalative binding of 2-0-2, 2-1-2, 2-2-2 and 2-3-2, with the representative model oligodeoxynucleotide duplexes d(CGGCG) · d(CGCCG), $d(CGATCG)_2$, d(GCGCCG) · d(CGGCGC) and $d(CGCGCG)_2$. The model oligonucleotides are chosen in order to highlight and to evaluate the relative importance of the number of exclusion sites and of the alternating purine-pyrimidine or pyrimidine-purine preference of the drugs.

The choice of the JUMNA molecular mechanics procedure [1,2] is based on its ability to control DNA flexibility by means of a complete and proper set of helicoidal variables, instead of the commonly used set of cartesian coordinates. For the description of the nucleic acid structures the CURVES algorithm [9,10] was used.

The structural differences of the complexes formed between various of the oligonucleotides and the bis-intercalating substances 2-0-2, 2-1-2, 2-2-2 and 2-3-2 are determined in this study and their possible relation to the modulation of activity of the drug compounds discussed.

2. Methodology

The JUMNA procedure, in its version adapted to take into consideration the presence of a (noncovalently) bound ligand [11], and already employed in our previous work [3,4] has been described elsewhere in detail [1,2]. In order to represent the effects of interaction between the DNA fragment and the drug, all torsional variables in drug and DNA have been freed during minimization. The values of the sigmoidal-shape dielectric function parameters and those of the phosphate unit electrostatic charges have been scaled to mimic the effects of solvent and of counterion condensation particular to the B form of DNA, and are as before [12,13]. The atomic charge densities of the ligands and the DNA fragments were computed using the previously reported Hückel-Del Re parametrization [12,13]. The DNA-ligand system did not contain counterions. The molecular models of the drugs were generated from that of ditercalinium by adding the necessary methylene groups between the linking chain piperidinium rings. The procedure for finding acceptable initial binding positions consisted in: (i) creating the intercalation sites by setting a spacing along the helical axis (Z) of 6.8 Å and a winding (W) of 10° between the corresponding base-pairs; (ii) setting the values of Z and W to 3.38 Å and 45° for the exclusion sites, and of tilt (T) and propellor (P) to 0° for all bases; (iii) locking these variables at these values and minimizing in the absence of the ligand; (iv) obtaining a partially relaxed structure in which all other variables were

free to vary, including backbone torsions; (v) binding or 'docking' of the ligand: creating preliminary binding positions by docking to the oligonucleotide a ligand whose torsion angles had been adjusted to form an antiparallel intercalating structure in which the chromophores were oriented in opposite directions. For the molecular modeling an Evans & Sutherland PS390 raster graphic terminal was used together with the commercially available software package SYBYL [14].

The minimized structures were analyzed using the CURVES algorithm [9,10], which provides a rigorous description of an irregular nucleic acid segment. In this method the curvature of the segment and the variation of the helicoidal parameters of the bases are described simultaneously by a function which is then minimized to obtain the best global description of the structure.

The exclusion parameter n will be defined here as the number of internal exclusion sites created during the intercalating event. These sites are to be differentiated from the external exclusion sites, i.e., those sites located between intercalated drug molecules. At the time of the enunciation of the 'nearest neighbor exclusion model' principle by Crothers [15,16] and other workers [19] poly-functional intercalation was not referred to, and thus no allusion was made to the difference between internal and external excluded sites. The number of oligonucleotide base-pairs sandwiched between the planar chromophore moieties of a homogeneously intercalated polyfunctional ligand, i.e., one which intercalates always with the same number of exclusion sites n, becomes then $n+1$ (for homogeneous intercalation, $n_i = n_j$ for any drug molecules i and j). In the limit of saturation for homogeneous bis-intercalation the site-size parameter of Waring [20], i.e., the number of nucleotide pairs occupied by a bound drug molecule in the presence of one exclusion site between bis-intercalated ligands, should approach 5 for $n = 2$ and 6 for $n = 3$. The order of intercalation m of a polyintercalator corresponds to the number of intercalated chromophores. In such a way, polyfunctional intercalation may now be characterized, in the most general fashion, by its exclusion n and its order m. For example, for the bis-intercalated complexes 1 and 2 of table 1, $m = 2$ and, respectively, $n = 2$ and 3. These definitions become particularly useful for the case in which $m > 2$ [21] and if intercalation is inhomogeneous, i.e., if for a given intercalator, n is not the same either through one DNA complex or between DNA complexes ($n_i \neq n_j$). In that case, a sequence of digits for the values of n would suffice to describe uniquely the mode of intercalation. For example, a ligand may tris-intercalate asymmetrically such that two and three pairs are surrounded by the intercalating moieties; then $n_1 = 2$, $n_2 = 3$.

A complex, A, formed between an intercalating substance and a nucleotide is an *exclusion site isomer* of complex B if the ligand and the nucleotide are the same in both complexes and $n(\mathrm{A}) \neq n(\mathrm{B})$, i.e., the number of exclusion sites is different in each case. Additionally, two different intercalating substances IA and IB are *intercalomers* of each other if there is a situation for which $n(\mathrm{IA}) = n(\mathrm{IB})$ and $m(\mathrm{IA}) = m(\mathrm{IB})$. Exclusion site isomerism is a reflection of the intercalative capacities of a ligand, such as in complexes 1 and 2 (table 1), compounds 2-3-2 and 2-2-2 are themselves intercalomers as reflected in their ability to bis-intercalate to CGATCG with, for instance, $n = 3$ (complexes 2 and 4, respectively).

3. Results and discussion

Table 1 presents a compilation of the DNA-ligand stabilization energies for selected optimal complexes obtained in the series of major groove bis-intercalators ($m = 2$) 2-0-2, 2-1-2, 2-2-2 and 2-3-2, to the four model hexanucleotides indicated above. As a consequence of intercalation into the major groove side, the concave edges of the chromophore rings in all complexes appear oriented toward this groove. The total stabilization energy of a system E_s (column 5) composed of a nucleotide fragment and a ligand is given by the sum of all intermolecular E_{INTER} (column 4) and intramolecular ΔE_{DNA} (column 2), ΔE_{LIG} (column 3) interactions. ΔE_{DNA} and ΔE_{LIG} represent energy changes with respect to the free reference states of the DNA fragment and the ligand, respectively. Energy minimization was carried out in the absence of any distance constraints. As minor

groove intercalative binding was previously shown theoretically [3,4] and experimentally [8] to be much less favorable in the case of an alternating CG sequence, only intercalation through the large groove is dealt with in this study.

The second, fourth and twelfth complexes of table 1 have been already characterized experimentally by solution NMR studies [8]. Complexes 1 and 2 constitute a situation in which the relative ability of the drug to intercalate to the same hexanucleotide is measured in terms of the exclusion parameter ($n = 2$ and 3, respectively) and the local sequence at the intercalation site. The same applies for the following complexes: 3 and 4; 5 and 6; 7 and 8. As shown by the values of the overall energy balances E_s, in all intercalation isomers (1 and 2; 3 and 4; 5 and 6; 7 and 8) the complexes that intercalated following the alternating 5′-pyrimidine-purine-3′ sequence for both chromophores were favored over those that did not. Thus, complex 4 is favored over complex 3 by 23.5 kcal; complex 5 is more stable — by 17.0 kcal — than its intercalation isomer, complex 6. In its turn, complex 8 shows an increased stability of 24.4 kcal with respect to its intercalation isomer complex 7. When 2-3-2 is the ligand, the stabilization of complex 1 over complex 2 amounts to 24 kcal. Complex 8 is slightly more stable than complex 4 due to the presence of the central dCpdG sequence.

If we assume that the differences in total solvation energies of complexation between complexes that contain the same nucleic base composition are of the same order, we observe the following: for complex 5 and complex 8, in which the step of intercalation dCpdG is the same, the complex with $n = 3$ is slightly favored over that with $n = 2$. This follows as well for the pair of complexes 6 and 7. Thus, bent bis-intercalated DNA complexes appear to be more stable than straight ones.

By taking the more stable of each complex in each of the four pairs of complexes (1 and 2; 3 and 4; 5 and 6; 7 and 8), we have, in order of relative decreasing stabilities: complex $8 > 4 > 5 > 2 \gg 10 \gg 12$. We note, then, that complexes with 2-2-2 as the ligand are, in general, slightly more stable than those with 2-3-2 as the ligand. The latter are, in turn, more favored than the 2-0-2 complexes. This is in agreement with the affinity constants of these compounds for DNA [22].

Investigation of the major groove intercalative mode of 2-2-2 to CGATCG (complex 4) indicates that, as in the ditercalinium/CGCG complex [4], complexation is stabilized essentially by a hydrogen bond between the side chain piperidinic hy-

Table 1

Summary of the energy terms for the optimal major groove bis-intercalating complexes of ditercalinium (2-0-2), and its three derivatives 2-1-2, 2-2-2 and 2-3-2 (see fig. 1) with selected model oligonucleotides (values in kcal/mol)

Complex [a]	n [b,d]	ΔE_{DNA}	ΔE_{LIG}	E_{INTER}	E_s	∂E_s [c]
(1) 2-3-2/CG ATC G	2	56.6	11.4	−185.3	−117.3	29.7
(2) 2-3-2/C GATC G	3	63.0	11.0	−215.3	−141.3	5.7
(3) 2-2-2/CG ATC G	2	54.8	2.0	−180.3	−123.5	23.5
(4) 2-2-2/C GATC G	3	66.3	4.5	−217.8	−147.0	0.0
(5) 2-2-2/GC GCC G	2	52.8	2.9	−199.5	−143.8	3.2
(6) 2-2-2/G CGCC G	3	67.2	4.9	−198.9	−126.8	20.2
(7) 2-2-2/CG CGC G	2	63.4	3.5	−192.1	−125.2	21.8
(8) 2-2-2/C GCGC G	3	63.2	5.2	−218.0	−149.6	−2.6
(9) 2-1-2/C GGC G	2	73.9	7.3	−174.6	−93.4	53.6
(10) 2-0-2/GC GC GC	1	70.6	3.1	−195.8	−122.1	24.9
(11) 2-0-2/C GGC G	2	95.9	4.0	−211.4	−111.5	35.5
(12) 2-0-2/C GA TCG	1	64.2	1.7	−171.9	−106.0	41.0

[a] A space between two bases denotes an intercalation site.

[b] n: number of exclusion sites.

[c] ∂E_s: energy changes with respect to complex 4.

[d] m, the number of intercalated chromophores is equal to 2 in all cases, except complex 9, where $m = 1$.

drogens and N7 of the respective vicinal internal guanines, Gua2 and Gua8 (see table 2 for H-bonding data). Proximity of these hydrogens to O6 of the same guanine bases suggests the existence of a bifurcated hydrogen bond. Indeed, several alternate conformations are likely to be valid representations of the low energy conformational states that are part of the dynamics of the structure. The indolic hydrogen D7 is located in the minor groove side and finds itself in the vicinity of O1′ of the cytidine deoxyribose of the respective intercalation site, as was also true for the ditercalinium complex. The acceptor---H---donor angle in this case is 111°; nevertheless, by assuming a nearly tetrahedral geometry for O1′, the D7---(lone pair of O1′)---O1′ angle is 154°, i.e., nearly colinear. These proposed hydrogen bonds are in agreement with the slow rate of exchange with the D_2O solvent observed for these protons by NMR [8]. Intramolecularly, the drug causes an approach, on the major groove side, of O4 of thymine 4 to H2N4 of the contiguous cytosine 5 (see table 2); nevertheless, all Watson-Crick hydrogen bonds are preserved. The sugar puckering pattern in the 5′-3′ direction is, for either strand, C2′-*exo*–C3′-*exo*–C3′-*exo* (or C2′-*endo*)-O1′-*endo*–C3′-*endo*–C2′-*endo*, indicating the existence of an alternating pattern for the sugars surrounding the intercalation sites.

Complex 2 (molecular graphics image not shown, but similar in conformation to complex 4) shows a slight departure from exact two-fold symmetry due to the particular arrangement of the central four C-C bonds of the linking side chain. This was not directly observed by NMR; nevertheless, in the ^{1}H-NMR spectra, due to a shorter lifetime the resonance linewidths for the 2-3-2 complex were broader than those in the 2-2-2/CGATCG complex. Several relevant interatomic proton-proton distances and hydrogen-bonding angles for complex 4 are listed also in table 2.

In table 3 we list the conformational states adopted by the glycosidic, sugar and phosphate backbone torsions of the representative optimal major groove complexes 3–7. We observe that, in general, the values of the backbone torsions that belong to equivalent segments of the chain backbone all fall in the same ranges. This is in line with the studies of Olson and co-workers [23,24] who have shown that a large number of torsional arrangements of the chain backbone may exist for a given base-pair morphology, but that on the basis of energy only a few of those arrangements are preferred.

Table 2

(a) H-bond distances (in Å) and the corresponding donor-hydrogen-acceptor angles (in °) for the 2-2-2/C GATC G complex (no. 4 in table 1)

Atom A	Atom B	Distance A–B (Å)	Atom C	Angle C-B–A (°)
Thy 4 O4	Cyt 5 N2N4	2.9	Cyt 5 N4	107.2
Gua 2 O6	H pip	3.0	N pip	164.4
Gua 2 N7	H pip	2.0	N pip	108.0
Sug 6 O1′	D7	2.6	N7 drug	110.6
Sug 6 O1′	Sug 6 lone pair of O1′	–	D7	153.9

(b) Selected non-exchangeable interproton distances for the 2-2-2/C GATC G complex

Atom A	Atom B	Distance A–B (Å)
Thy 4 H2C5	-OCH_3 [a]	4.0 [c]
Cyt 5 HC5	-OCH_3 [a]	3.7 [d]
Gua 2 HC8	Hpip	3.4 [c]
Gua 2 HC8	Hc	5.5 [c]
Gua 2 HC8	Hd	4.0 [c]
Gua 2 HC8	Hd′	2.7 [c]
Gua 2 HC8	Hc′	3.9
Thy 10 H2C5 [b]	Hb	5.2
Thy 10 H2C5	Hc	4.1
Thy 10 H3C5 [b]	Hc	3.9
Thy 10 H3C5 [b]	Hd	5.2
Thy 4 H3C5 [b]	$H_{1'}$·II	4.9
Thy 4 H3C5 [b]	$H_{1'}$	4.9
Thy 10 H3C5 [b]	$H_{1'}$·II	4.9

[a] When oriented toward the internal cytosine base (Cyt 5). Averaged over H1, H2, H3. From Ref. 8; [b] Not seen due to overlap with $H_{2'}$, $H_{2''}$ or other protons; [c] Small observed NOE (4–5 Å separation); [d] Medium observed NOE (3–4 Å separation).

3.1. Unwinding angles

Table 4 lists the combined-strand average unwinding angles measured with respect to the corresponding relaxed oligomer (see ref. 9 for definitions) for each of the sites in the major groove

Table 3

Conformational states of backbone and sugar torsions of complexes 3–8

Torsion angle definitions are as follows: c, 0±30°; t, 180±30°; g^+, 60±30°; g^-, 60±30°; −ac, −120±30°; anti, 0–90° for the glycosidic bond; N, 288–72°, S, 108–252°; E, 72–108° for the sugar pucker. Torsions of ligand 2-2-2 in complex 4: $\tau 1 = +ac$, $\tau 2 = g-$, $\tau 3 = g-$, $\tau 4 = g-$, $\tau 5 = t$, $\tau 6 = t$ where $\tau 1$: C_9-C_{10}-O-C_f, $\tau 2$: C_1-N_2-C_a-C_b, $\tau 3$, N_2-C_a-C_b-N, $\tau 4$: C_a-C_b-N-C_c', $\tau 5$: $C_{d'}$I-C_eI-C_fII-C_fII, $\tau 6$: C_eI-C_fI-C_fII-C_eII.

Torsion angle						
γ (C5′-C4′)	∂ (C4′-C3′)	ε (C3′-O3′)	ζ (O3′-P)	α (P-O5′)	β (O5′-C5′)	
Base pair			Complex 3			
C1/G12	−/g+	N/S	t/−	g−/−	g−/−	t/−
G2/C11 [a]	g+/t	N/S	t/t	−ac/−ac	t/g−	t/t
C3/G10	t/g+	S/E	t/t	g−/g−	g−/t	t/t
G4/C9	g+/g+	S/S	t/t	−ac/−ac	g−/g−	t/t
C5/G8	g+/t	E/S	t/t	g−/g−	t/g−	t/t
G6/C7 [a]	t/−	S/E	−/t	−/−ac	−/−ac	−/t
			Complex 4 (dyad symmetry)			
C1/G12 [a]	−/t	E/S	t/−	−ac/−	−ac/−	t/−
G2/C11	t/g+	S/E	t/t	g−/g−	g−/t	t/t
A3/T10	g+/g+	S/E	t/t	−ac/g−	g−/g−	t/t
T4/A9	g+/g+	E/S	t/t	g−/−ac	g−/g−	t/t
C5/G8	g+/t	E/S	t/t	g−/g−	t/g−	t/t
G6/C7 [a]	t/−	S/E	−/t	−/−ac	−/−ac	−/t
			Complex 5			
G1/C12	−/g+	N/S	−ac/−	g−/−	g−/−	t/−
C2/G11 [a]	g+/t	S/S	t/t	−ac/−ac	t/g−	t/t
G3/C10	t/g+	S/N	t/t	−ac/g−	g−/t	t/t
C4/G9	g+/g+	S/S	t/t	−ac/−ac	−ac/g−	t/t
G5/C8	g+/t	N/S	t/t	g−/g−	t/g−	t/t
C6/G7 [a]	t/−	S/N	−/t	−/−ac	−/−ac	−/t
			Complex 6			
G1/C12 [a]	−/t	N/S	t/−	g−/−	t/−	−ac/−
C2/G11	t/g+	N/N	−ac/−ac	g−/g−	g−/t	t/t
G3/C10	g+/g+	S/N	t/t	−ac/g−	−ac/g−	t/t
C4/G9	g+/g+	N/S	t/t	g−/−ac	g−/g−	t/t
C5/G8	g+/t	N/S	t/t	g−/c	t/−ac	t/t
G6/C7 [a]	t/−	S/N	−/t	−/−ac	−/t	−/t
			Complex 7			
C1/G12	−/g+	N/S	t/−	g−/−	g−/−	t/−
G2/C11 [a]	g+/t	N/S	t/t	−ac/−ac	t/g−	−ac/t
C3/G10	t/g+	N/E	−ac/t	g−/−ac	g−/t	t/t
G4/C9	g+/g+	S/E	t/t	−ac/−ac	g−/g−	t/t
C5/G8	g+/t	N/S	t/t	g−/g−	t/g−	t/t
G6/C7 [a]	t/−	S/N	−/t	−/−ac	−/−ac	−/t

Notes:

[a] Intercalation site. χ falls in the anti region for all complexes. For sugar pucker and torsion angle definitions and conventions see text. Torsions for complex 8 virtually as in complex 4. A dash (−) denotes that a given torsion angle is not defined for that nucleotide unit. A diagonal (/) separates the two bases of a base-pair.

complexes of table 1. It can be seen that when the number of exclusion sites increases, the average total unwinding increases. Thus, complexes 2, 4, 6 and 8 with $n = 3$ have the largest unwinding angles (52–59°). These are followed by complexes 1, 3, 5 and 7 for which $n = 2$ (37–48°). Complex 9 is pseudobis-intercalated because one of its chromophores is significantly shifted away from the base pair lodge into the major groove. This is due to the particular V-shaped conformation of 2-1-2 [6,25]. Note that, in general, purine-pyrimidine and purine-purine intercalation sites are associated with smaller unwinding angles than the pyrimidine-purine sites.

As was the case for ditercalinium [4], the total theoretical DNA unwinding angle generated by the dimers is more than twice that of the corresponding monomers, and larger than DNA unwinding angles found in solution for the corresponding dimers (table 4). However, as already shown by calculations for ditercalinium [4], due to an *over* winding effect at the ends of the complexed oligonucleotides, the total unwinding was reduced upon addition of terminal nucleotide pairs. We can then infer that the total unwinding in the complexes studied here would also be diminished if the length of the DNA fragment per intercalated drug were to be increased. Thus, with respect to the experimentally determined unwinding of plasmid pUC13 DNA (26.1° for 2-2-2, for example [6]), it should be possible, in the light of calculations such as this, to estimate the magnitude of the contribution to the total unwinding of the supercoiled DNA by the bases adjacent to the intercalation sites. Additional effects, such as secondary binding (groove binding) and pseudointercalation, will also combine to produce a drastic reduction in the total average unwinding per bound drug while at the same time resulting in properties that mimic classical intercalation. The effects of groove binding are clear from the theoretical work of Lavery et at. [26], in which the introduction of antibiotic ligands into the minor groove of DNA produces a rather small unwinding of 1°. Experimental evidence to the same effect may be found in the work of Damaschun et al. [27]. On the other hand, it is not obvious how, experimentally, the substitution of the indolic hydrogen at N7 by a single methyl group may affect the unwinding so much. For example, for 2-0-2 the unwinding changes from 20.3 to 52.8°; for 2-1-2, from 23.7 to 30.7°; and for 2-2-2, from 26.1 to 21.8° [6]! Calculations in the presence of a methyl group at N7 (not shown here) do not show changes of such magnitude in the total unwinding.

Thus, we may conclude that, for a given experi-

Table 4

Negative values correspond to overwinding. Experimental values of supercoiled DNA unwinding determined by change in electrophoretic migration of plasmid pUC13 DNA in agarose gel [6]. For 2-1-2, 23.7°; 2-2-2, 26.1°; 2-3-2, not determined.

Complex	2-Strand average unwinding (°) (Site)						Bending angle θ (°)	Direction angle ϕ (°)
	I	II	III	IV	V	Total		
1	2.9	12.3 [a]	−6.5	4.9	26.0 [a]	39.6	5.9	−123.3
2	27.9 [a]	5.3	−4.2	4.5	25.2 [a]	58.7	27.2	−195.8
3	2.3	14.0 [a]	−5.4	5.0	26.1 [a]	42.0	8.8	−153.6
4	27.7 [a]	3.4	−4.0	2.9	26.2 [a]	56.2	31.3	−183.0
5	2.1	15.2 [a]	−1.0	−0.9	21.8 [a]	37.2	5.4	−192.7
6	14.0 [a]	7.7	0.5	11.9	21.2 [a]	55.3	53.4	−165.4
7	6.0	3.1 [a]	7.1	6.7	25.1 [a]	48.0	16.5	−153.8
8	29.6 [a]	−2.1	−0.9	−0.1	25.0 [a]	51.5	29.7	−182.9
9	12.7 [a]	4.2	6.7	12.1 [a]	–	35.7	11.3	−85.4
10	−2.8	20.7 [a]	−9.6	23.7 [a]	−2.5	29.5	15.2	2.1
11	20.1 [a]	3.9	5.7	24.7 [a]	–	54.4	16.7	−157.8
12	31.0 [a]	−5.4	16.1 [a]	−0.4	9.5	50.8	5.0	−7.4

[a] Intercalation site.

mental measurement, the value of n may not be unique for a given ligand and the associated nucleotide sequence. This is reflected, for instance, in the 6° unwinding difference between intercalation isomer complexes 6 and 7 whose stabilization energies are virtually identical. Averaging the total unwinding of the three favored complexes of 2-2-2 (complexes 4, 5 and 8) gives a value of 48.3°.

That there is more than the simple phenomenon of intercalation intervening may be also reflected in the significant variation of the value of the slope s of the DNA lengthening experiment plots. This value ranges from 1.83 in the case of N7-methyl substituted 2-2-2, to 2.91 in the case of N7-methyl substituted 2-0-2 [6].

The effects of a pyrimidine-purine vs purine-pyrimidine sequence on the unwinding angle of an intercalated step may be seen, for example, upon comparing site II of complexes 5 and 7. In the latter protons H1N4 and H2N4 of Cyt 3 come in close contact with one of the Hd protons of the drug. This results in rather large propeller (36°) and buckle (17°) distortions for base Cyt 3 and in the base-pairs belonging to the dG-dC site being practically unwound (3°).

3.2. DNA bending

The term bending will be used here to refer to a curvature induced on the DNA fragment by an external agent, in this case the intercalating substance; the term curvature is used to mean the inherent curvature of the oligonucleotide, which has been shown to be sequence-dependent (ref. 28 and references therein). The angle θ, defined as the angle between the mean unit vectors of the helical axes of the first and last base-pair is a measure of the overall degree of curvature of the nucleic acid structure [9]. The angle ϕ measures the angular direction of the curvature with respect to the dyad axis of a virtual base-pair located at the center of the DNA fragment and having a twist intermediate to the twists of the base pairs surrounding it. Values of ϕ of 0, 90, ± 180 and $-90°$ correspond to bending toward the minor groove, 3′-5′ strand, major groove or 5′-3′ strand, respectively.

Complexes 1, 3, 5 and 7 turn out to show relatively small bending deformations to the naked eye (see the molecular graphics representation of complex 3 in fig. 2) and to the formal mathemati-

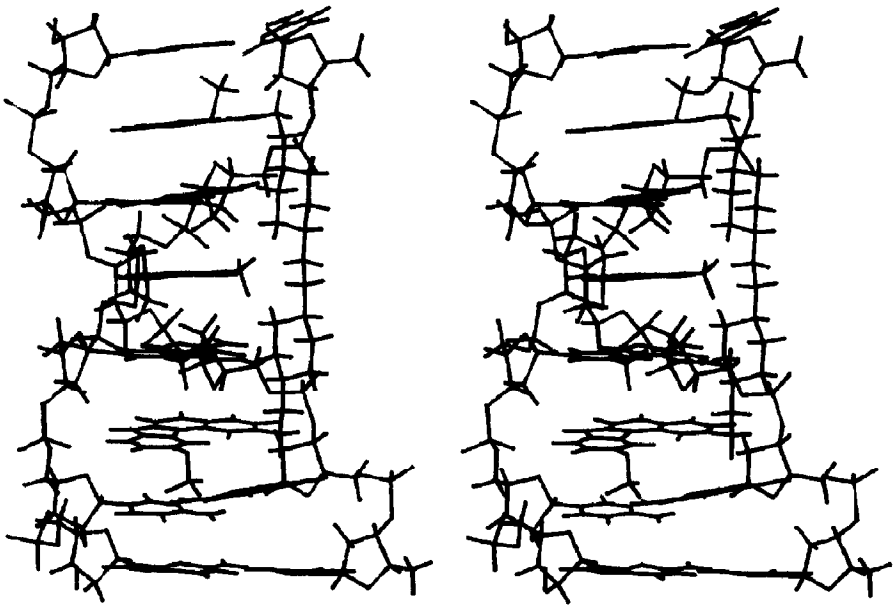

Fig. 2. Relaxed stereoscopic view (from 3′-5′ strand) of complex 3 (2-2-2/(dCG ATC G)$_2$) with the linking chain located in the major groove.

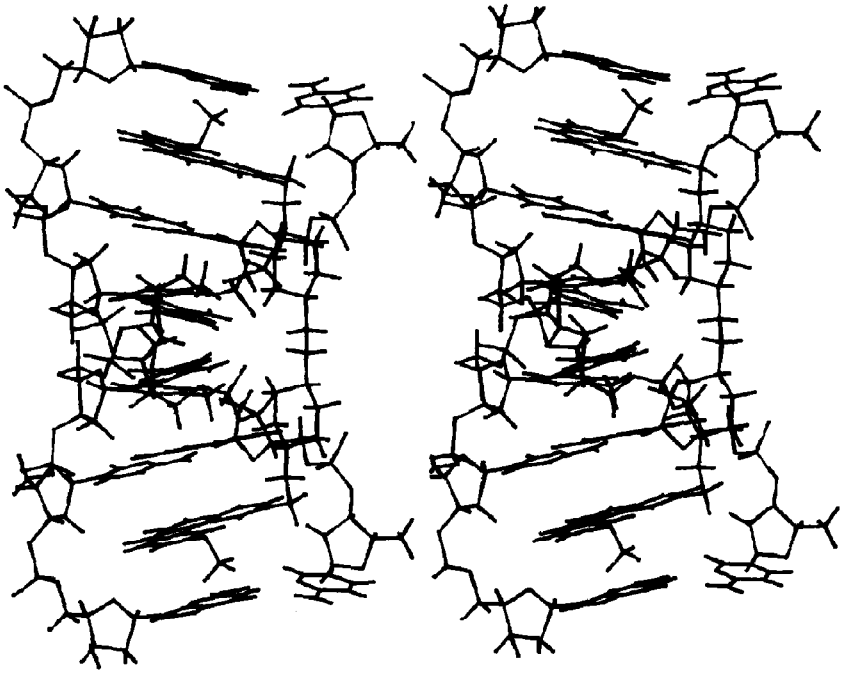

Fig. 3. Relaxed stereoscopic view (from 3′-5′ strand) of complex 4 (2-2-2/d(C GATC G)$_2$) with the linking chain located in the major groove.

cal analysis of the optimal global helical axis system using CURVES [8,9] in which virtual ends of canonical B-DNA have been added to the sequence; values of the corresponding bend angles θ are listed in the next to the last column of table 4. CURVES gives only a slight degree of bending, i.e., 8.8° for complex 3. Complex 4, represented in fig. 3, shows instead a marked bending toward the major groove. The bending of this complex with $n = 3$ amounts to 31.3° (table 4). This can be compared to the 15.2° bending for the ditercalinium/GCGCGC complex 10 with $n = 1$. The overall structure of complex 8 is almost identical to the 2-2-2/CGATCG complex 4. The bending in complex 4 occurs mainly at junction 3, i.e., between base-pairs 4 and 3 (fig. 1). The highest values of the bending angle are attained by complexes 6, 4 and 8 (2-2-2 with $n = 3$), followed by complex 2 (2-3-2 with $n = 3$). The complexes with $n = 2$ come last.

When looking at the relations between the total unwinding angle and the angle of bending for complexes of the same chain length (complexes 1–8, 10 and 12) we observe that a bending of the nucleotide will be accompanied by an unwinding. The converse is also true.

Selecting complexes 10 and 12 for 2-0-2, 9 for 2-1-2, 4, 5 and 8 for 2-2-2, and 2 for 2-3-2, we note that a comparison of the degree of bending to their antitumoral activity in vivo indicates (i) that the direction of bending as measured by the angular direction ϕ changes from a bending toward the minor groove in the case of 2-0-2 to a bending toward the major groove for 2-3-2; (ii) that an increased overall bending is related to a decrease in the activity of the intercalating dimer (table 5 and fig. 4).

This as yet inconspicuous relationship between the degree and direction of bending of the complexed DNA and the activity of the drug provide a quantitative model for the action of ditercalinium and its derivatives. Included in the distortions on the DNA helix recognized by the uvrA product and necessary for binding and the formation of a

Table 5

Complex	Activity [a] (ligand)	Averaged bending angle θ (°)	Averaged direction angle ϕ (°)
10, 12	182 (2-0-2)	10.1	4.8
9	175 (2-1-2)	11.3	−85.4
4, 5, 8	143 (2-2-2)	22.1	−186.2
2	ns [b] (2-3-2)	27.2	−195.8

[a] Activity against murine leukemia L1210 tumors expressed as increase in mean life span of the test (T) and control (C) animals (T/C %).
[b] Non-significant.

repair complex [29,30] are those of a local nature such as tip (i.e., rotation about DNA's long axis), displacement along the dyad axis, displacement along the long axis shift, and buckle. These additional base distortions in the form of local deviations from canonical Watson-Crick B-DNA structure are developed in section 3.3.

3.3. Helicoidal parameters

For definitions, conventions and illustrations of the set of helicoidal parameters used in this section, see refs. 9 and 29.

Other classes of deformations at the nucleotide base-pair level accompany the bending. Thus, for complex 4 there is a collective motion of all base-pairs toward the minor groove, being greatest (0.90 Å) for base-pairs 2 and 5; a slight displacement of base-pairs 2,4 and 6 toward the 3′-5′ strand (0.1–0.2 Å), and an equivalent one for base-pairs 1, 2 and 3 in the opposite direction; a negative buckle, i.e., a buckle in the 3′-direction of the 5′-3′ strand, of base-pairs 1, 2 and 4, reaching a maximum of almost 12° for base-pair 1. For base-pairs 3, 5 and 6 a positive buckle of the same magnitude is observed. In addition, a roll wedge of junctions 2–4 produces a compression of the major groove. Present are also negative inclinations of −9 and −5° for base-pairs surrounding the intercalation sites; and propellers of −16° for the central dAdT and dTdA base-pairs and of 18° for the terminal pairs (data not shown). For complex 10, the displacement of base-pairs 2 and 5 is rather toward the major groove; base-pairs 2 and 3 are slid to the 3′-5′ strand, whereas 4 and 5 are slid to the other strand; buckles of base-pairs surrounding the intercalated aromatic cycles observe the same trends as in the case of complex 4; present is a slight roll wedge of junction 3 toward the minor groove; and inclination and propeller have the same trends as in complex 4.

Departures of the canonical form of B-DNA such as those just mentioned are not limited to bent structures. They may also exist in the presence of very small or no bending, as is the case of complex 5 (data not shown).

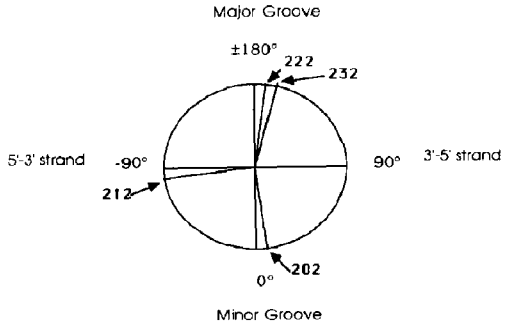

Fig. 4. Diagram showing the average angular direction of bending for ditercalinium (2-0-2) and its derivatives (2-1-2, 2-2-2 and 2-3-2).

4. Conclusion

In the present theoretical study we have derived the preferred binding configurations of a series of complexes formed by major groove bifunctional intercalation of a number of derivatives of ditercalinium to a number of representative model oligonucleotides. The derivatives varied only in the length of the linker chain. For the complexes treated in this work, including three for which ^{1}H- and ^{31}P-NMR studies have been carried out, we have described specifically the alterations induced by the drug on the DNA fragment.

After energy optimization the structures of the resulting complexes were found to be compatible

with the set of intra- and intermolecular proton-proton distances obtained from NMR NOEs. The energy analysis pointed to a binding in which intercalation into an alternating 5′-pyrimidine-purine-3′ sequence is the priority event upon complexation. Depending then on the base sequence, the number of exclusion sites n varied. Those complexes for which $n = 3$ presented an increased bending of the DNA minihelix with respect to the structures with $n < 3$. When a drug induced a marked bending on the DNA fragment, the bending was toward the major groove. Nevertheless, in all cases the DNA fragment remained in the B form. The calculations enabled us also to predict the preferential binding sites of the binuclear ligands of the ditercalinium family for a given oligonucleotide.

The distribution of the unwinding angles of the complexes indicated an association between unwinding and bending, i.e., both will increase or decrease together. This correlation is perhaps of a more general character and may occur during any other type of situation involving bending.

We have also established that the observed antitumoral activity of the drug is associated to a bending of the DNA fragment to which it intercalates. In the case of an active drug (ditercalinium), the bending is toward the minor groove; for a drug with small or no antitumoral activity (2-2-2), the bending is of a larger magnitude and toward the major groove. Additional distortions of a local nature are present, such as tip, twist, buckle, etc., of the nucleotide base-pairs. Nevertheless, the small differences found between complexes for these variables do not seem to provide an explanation for the difference in activities observed.

The type of interactions studied here are very relevant in the search for more effective polyfunctional antitumoral agents in the family of intercalators of ditercalinium. Thus, chemical modifications to the ditercalinium molecule could be proposed that would accentuate its binding affinity to DNA. For example, a quaternized nitrogen substituent in *meta* position to the piperidinium nitrogen of the linker chain is a possible candidate to be tried, or, for that matter, the addition of a small group capable of establishing a hydrogen bond with O6 of the internal guanines and that at the same time increases the solubility in water of the drug. Based also on what we have learned about the type of deformations caused by the drugs on the DNA molecule and the relation to their biological activity, a ligand that accentuates the degree of minor groove bending would be expected to ameliorate its activity. Independently, a rather 'short' bis-intercalator such that the interchromophoric distance of 3.4 Å, enough to 'sandwich' only one nucleotide pair between chromophores, and with no specific sequence preference, could be envisaged to test the nearest neighbor exclusion principle.

The forces present in the model systems of the type studied here could also serve as a model to understand higher levels of interaction such as the binding mechanisms occuring in protein-nucleic acid interactions. For example, one form of contact between aromatic side chain amino acids in proteins and nucleotides takes place through stacking after intercalation of the aromatic moieties of the particular amino acids between the concerned DNA nucleotide pairs. The slow kinetics of formation of oligonucleotide-oligopeptide complexes in which the peptides contain aromatic amino acids support the insertion of the aromatic rings of aminoacids between the bases of the oligonucleotide [32,33]. The major mode of binding of single-strand binding (SSB) proteins also appears to require insertion of aromatic side chains between the nucleic acid base-pairs [34]. As is the case of polyintercalating compounds, protein ligands cover several nucleotide residues. The presence of excluded binding sites is reflected in the complex equilibrium distribution that takes place. For instance, the absence of mobility on the millisecond time scale of gene 5 protein, an SSB protein, is due to the intercalation of its aromatic side chains in the 4-nucleotide region which it covers upon binding [35].

Finally, ligand-induced changes of the DNA structure can be detected by looking at the orientation of the large anisotropic DNA molecule. Measurements of rotation time constants of an 80 base-pair DNA-cyclic AMP complex indicate that its formation induces strong *bending* around the activator [36,37].

Acknowledgements

The authors wish to thank both Professor C. Garbay-Jaureguiberry, and Dr M. Delepierre, for many fruitful discussions, and the latter for providing valuable NMR data information. We thank C. Dupuis for typing the manuscript.

References

1 R. Lavery, in: Unusual DNA structures, eds S. Harvey and R. Wells (Pergamon, New York, 1988) p. 189.
2 R. Lavery in: DNA bending and curvature, eds W.K. Olson, M. Sundaralingam, M. Sarma and R.H. Sarma (Adenine Press, New York, 1988) p. 191.
3 R. Maroun and N. Gresh, Biopolymers 4 (1989) 835.
4 R. Maroun, M. Delepierre and B.P. Roques, J. Biomol. Struct. Dyn. 7 (1989) 607.
5 L.P.G. Wakelin, Med. Res. Rev. 6 (1986) 275.
6 C. Garbay-Jaureguiberry, P. Laugâa, M. Delepierre, S. Laalami, G. Muzard, J.B. Le Pecq and B.P. Roques Anti-Cancer Drug Design 1 (1987) 323.
7 D. Pelaprat, A. Delbarre, I. Le Guen, B.P. Roques and J.B. LePecq, J. Med. Chem. 23 (1980) 1336.
8 M. Delepierre, R. Maroun, C. Garbay-Jaureguiberry, J. Igolen and B.P. Roques, J. Mol. Biol. 210 (1989) 211.
9 R. Lavery and H. Sklenar, J. Biomol. Struct. Dyn. 6 (1988) 63.
10 R. Lavery and H. Sklenar, J. Biomol. Struct. Dyn. 6 (1989) 655.
11 K. Zakrzewska and B. Pullman, J. Biomol. Struct. Dyn. 5 (1988) 1043.
12 R. Lavery, K. Zakrzewska and A. Pullman, J. Comput. Chem. 5 (1984) 363.
13 K. Zakrzewska and A. Pullman, J. Comput. Chem. 6 (1985) 265.
14 SYBYL version 5.1, Tripos Associates, St. Louis, MO, U.S.A.
15 D.M. Crothers, Biopolymers 6 (1968) 575.
16 D.M. Crothers, in: Physical chemistry of nucleic acids, eds V.A. Bloomfield, D.M. Crothers and I. Tinoco, Jr (Harper and Row, New York, 1974) p. 406.
17 J.D. McGhee and P.H. von Hippel, J. Mol. Biol. 86 (1974) 469.
18 L.P.G. Wakelin and M.J. Waring, Biochem. J. 157 (1976) 721.
19 M.J. Waring, in: The molecular basis of antibiotic action, eds E.F. Gale, E. Cundliffe, P.E. Reynolds, M.H. Richmond and M.J. Waring (Wiley, London, 1972) 2nd Edn, p. 173.
20 M.J. Waring, in: Drug action at the molecular level, ed G.C.K. Roberts (Macmillan, London, 1977) p. 167.
21 P. Laugâa, J. Markovits, A. Delbarre, J.-B. LePecq and B.P. Roques, Biochemistry 24 (1985) 5567.
22 C. Garbay-Jaureguiberry, C. Esnault, M. Delepierre, P. Laugâa, S. Laalami, J.B. Le Pecq and B.P. Roques, Drugs Expl. Clin. Res. 13 (1987) 353.
23 E.R. Taylor and W.K. Olson, Biopolymers 22 (1983) 2667.
24 A.R. Srinivasan and W.K. Olson, J. Biomol. Struct. Dyn. 4 (1987) 895.
25 P. Laugâa, M. Delepierre, P. Léon, C. Garbay-Jaureguiberry, J. Markovits, J.B. LePecq and B.P. Roques, in: Molecular mechanisms of carcinogenic and antitumor activity, eds C. Chagas and B. Pullman (Pontificia Academia Scientarum, Vatican City, 1987) p. 275.
26 R. Lavery, K. Zakrzewska and B. Pullman, J. Biomol. Struct. Dynam. 6 (1986) 1155.
27 H. Damaschun, G. Damaschun, C. Zimmer, J.J. Müller, R. Misselwitz, D. Zirwer, I.A. Zalenskaya and V.I. Vorob'ev, Stud. Biophys. 104 (1984) 272.
28 W.K. Olson, A.R. Srinivasan, R.C. Maroun, R. Torres and W. Clark, in: Unusual structures of DNA, eds R. Wells and S. Harvey (Springer, New York, 1988) p. 207.
29 B. Lambert and J.B. Le Pecq, Nucleic Acids Res. 3 (1988) 1063.
30 C.S. Downes, Nature 332 (1988) 208.
31 M. Randrianarivelo, K. Zakrzewska and B. Pullman, J. Biomol. Struct. Dyn. 4 (1989) 769.
32 D. Porschke, Nucleic Acids Res. 8 (1981) 1591.
33 D. Porschke and J. Ronnenberg, Biophys. Chem. 13 (1981) 283.
34 S.C. Kowalczykowski, D.G. Bear and P.H. von Hippel, The enzymes (1981) vol. 14, p. 373.
35 D. Porschke and H. Rauh, Biochemistry 22 (1983) 4737.
36 D. Porschke, in: DNA-ligand interactions, eds W. Guschlbauer and W. Saenger (NATO ASI Series, Plenum, New York, 1987) p. 85.
37 D. Porschke, W. Hillen and M. Takahashi, EMBO J. 3, (1984) 2873.